Environmental Science Processes & Impacts

PAPER

View Article Online
View Journal | View Issue

Cite this: *Environ. Sci.: Processes Impacts*, 2025, **27**, 1640

Kinetic multilayer models for surface chemistry in indoor environments†

Pascale S. J. Lakey and Manabu Shiraiwa *

Multiphase interactions and chemical reactions at indoor surfaces are of particular importance due to their impact on air quality in indoor environments with high surface to volume ratios. Kinetic multilayer models are a powerful tool to simulate various gas–surface interactions including partitioning, diffusion and multiphase chemistry of indoor compounds by treating mass transport and chemical reactions in a number of model layers in the gas and condensed phases with a flux-based approach. We have developed a series of kinetic multilayer models that have been applied to describe multiphase chemistry and interactions indoors. They include the K2-SURF model treating the reversible adsorption of volatile organic compounds on surfaces, the KM-BL model treating diffusion through an indoor surface boundary layer, the KM-FILM model treating organic film formation by multi-layer adsorption and film growth by absorption of indoor compounds, and the KM-SUB-Skin-Clothing model treating reactions of ozone with skin lipids in skin and clothing. We also developed the effective mass accommodation coefficient that can treat surface partitioning by effectively taking into account kinetic limitations of bulk diffusion. In this study we provide detailed instructions and code annotations of these models for the model user. Example sensitivity simulations that investigate the impact of input parameters are presented to help with familiarization to the codes. The user can adapt the codes as required to model experimental and indoor field campaign measurements, can use the codes to gain insights into important reactions and processes, and can extrapolate to new conditions that may not be accessible by measurements.

Received 13th September 2024
Accepted 30th October 2024

DOI: 10.1039/d4em00549j

rsc.li/espi

Environmental significance

Surface processes and reactions indoors are important due to high surface-to-volume ratios, influencing indoor air quality. Kinetic models can help us better understand how chemicals are generated, transformed and removed indoors. By making multiphase kinetic multilayer models available in this publication, research groups can apply and adapt them to address scientific questions and improve their understanding of their indoor experimental measurements.

1 Introduction

The concentrations of many gas-phase compounds indoors are significantly impacted by partitioning into surfaces and multiphase chemical reactions due to the high indoor surface-to-volume ratios indoors.[1–4] Consequently, understanding interactions of compounds with surfaces indoors is important as it impacts human exposure to these compounds.[5–8] Indoor surfaces consist of different materials such as glass, paint, wallboard, and fabrics. Organic films ranging from nanometers to several micrometers can also form on many indoor surfaces.[9–13] In the presence of people, human skin is an important surface due to ozonolysis reactions of skin lipids,[14,15] which lead to the generation of a variety of semi-volatile organic compounds (SVOCs) and subsequent gas-phase chemistry leads to the formation of OH radicals.[16] Other reactions which are known to occur in indoor surfaces include oxidation, hydrolysis, acid–base reactions, nitration and halogenation.[17] Surfaces can also act as reservoirs for compounds to effectively extend the lifetime of the compound indoors.[4,18–23] The partitioning of indoor compounds to surfaces depends on the volatility or the octanal–air partitioning coefficient (K_{oa}).[4,23,24] The phase state and viscosity of the surface film can also impact the uptake of compounds due to bulk diffusion limitations[25,26] and several studies have shown that indoor surface films can be viscous semi-solids.[27–30]

It is important to be able to model indoor multiphase chemistry using fundamental kinetic parameters such as diffusion coefficients, partitioning coefficients, accommodation coefficients, and reaction rate coefficients rather than empirical parameterizations.[31] Important unknown parameters can be

Department of Chemistry, University of California, Irvine, CA92697, USA. E-mail: m.shiraiwa@uci.edu

† Electronic supplementary information (ESI) available. See DOI: https://doi.org/10.1039/d4em00549j

constrained by model fitting to experimental data. The model can also be used to test hypotheses of reaction mechanism and mass transport processes to gain mechanistic and quantitative interpretation of experimental measurements. If measurements can be reproduced, then sensitivity tests can determine the most important processes and reactions in the model to identify a rate-limiting step. Alternatively, if experimental measurements cannot be reproduced with a reasonable mechanism and parameters, it indicates that there are missing reactions or processes which should be included until the cause of the trends are understood. Additionally, it is important to note that experiments are often performed under limited conditions and often with high concentrations to obtain high signal-to-noise ratios. Once the model has reproduced the measurements, the concentrations in the model can be reduced and extrapolated to more realistic conditions. The model can subsequently be used to suggest conditions that would be interesting to explore experimentally. Lastly, a comprehensive model can be used as a benchmark for comparison to more simple equations or parameterizations to understand the validity of these equations under different conditions.

A powerful and useful kinetic model framework was developed by Pöschl, Rudich and Ammann (PRA) by applying a flux-based approach to describe uptake to a surface.[32] Based on the PRA framework, Shiraiwa *et al.* developed the kinetic double-layer model of aerosol surface chemistry and gas-particle interactions (K2-SURF) to describe reversible adsorption and reactions at a surface.[33] The kinetic multi-layer model of aerosol surface and bulk chemistry (KM-SUB) was further developed, which includes a gas phase, near-surface gas phase, sorption layer, quasistatic layer, and a number of bulk layers to treat gas-phase diffusion, reversible adsorption, reversible partitioning, bulk diffusion and chemical reactions.[34] The multi-layer approach of the model enables concentration gradients in the bulk to be resolved as a function of time and the effect of phase state can be determined. Shiraiwa *et al.* subsequently developed the kinetic multi-layer model of gas-particle interactions in aerosols and clouds (KM-GAP) by treating the volume change of a layer in response to mass transport and chemical reactions so that particle growth and evaporation can be resolved.[35] Importantly, all of these models use fundamental physicochemical parameters.[34,36] Overall, these multi-layer kinetic models have many advantages over previous formulations like the resistor model, which has been widely applied to describe uptake coefficients. The resistor model has several critical assumptions including steady-state conditions, homogeneous mixing, first-order reactions and non-interacting compounds and processes;[37,38] while it can describe limiting cases when the system is dominated by a certain process, it cannot describe a system in transition kinetic regimes. Advantages of the kinetic multilayer models include the ability to treat (1) the dynamic evolution of the uptake coefficient and chemical composition, (2) the bulk concentration gradients of all compounds due to the inclusion of bulk layers, (3) an unlimited number of reactions which can be of any order and (4) interactions between compounds such as through chemical reactions or a change in physical properties such as viscosity as the condensed-phase composition evolves as products form.

The K2-SURF, KM-SUB and KM-GAP model were primarily developed for multiphase chemistry of aerosol particles and how the interplay between chemical reactions, phase state, and a range of fundamental kinetic parameters influence gas-particle interactions including gas uptake and secondary organic aerosol formation.[36,39–53] Within the Sloan modeling consortium of chemistry of indoor environments (MOCCIE),[31] this approach has now been adopted to investigate indoor chemistry with kinetic multilayer layer models having been adapted to describe interactions of indoor gaseous species with indoor surfaces. For example, K2-SURF has been used to reproduce measurements for adsorption of organic molecules on indoor-relevant surfaces, bridging measurements and molecular dynamics simulations to obtain an understanding of surface interactions in a molecular level.[33,54–56] Applications of KM-SUB and KM-GAP have revealed that diffusion limitations and surface crust formation retard uptake of molecules and product formation in indoor surface films.[34,35,57–59]

We have recently developed new kinetic multi-layer models that can specifically describe surface processes relevant in indoor environments. The kinetic multi-layer model of the boundary layer (KM-BL) describes mass transport and chemical reactions occurring in the indoor boundary surface layer.[60] We developed the kinetic multi-layer model of film formation, growth, and chemistry (KM-FILM) to simulate formation and growth of indoor surface organic films.[25] We then developed a simple effective mass accommodation coefficient (α_{eff}), which was first formulated for particle uptake,[61] and describes uptake of gaseous species to surface films by effectively accounting for diffusion limitations without the multilayer treatment.[26] This makes using the equation computationally much more efficient while good agreement with KM-FILM is obtained under most conditions. This α_{eff} approach and KM-FILM have been used to better understand the potential of surfaces to act as reservoirs as a function of K_{oa} and bulk diffusion coefficients.[25,26] We have developed the kinetic multilayer model of surface and bulk chemistry of the skin and clothing (KM-SUB-Skin-Clothing) to simulate ozone reactions with skin lipids including squalene and other unsaturated fatty acids in skin and clothing.[62] This model has also been used to understand the impact of relative humidity on the product yield and to gain a better understanding of this chemistry on indoor OH concentrations and reactivity.[16,63] Yields and uptake coefficients obtained from the model have been used as inputs to computational fluid dynamics (CFD) simulations to obtain a better understanding of the spatial distribution of ozone and ozonolysis products.[16,62,64]

Although kinetic multilayer models are useful in understanding the impact of partitioning, diffusion and multiphase chemistry on the uptake of compounds to surfaces, only a few codes have been released. We developed and released a user-friendly interface for K2-SURF and KM-SUB including the MATLAB codes which can be used for teaching or research purposes.[65] Milsom *et al.* developed and released MultilayerPy which is a framework for building and running KM-SUB and KM-GAP as well as optimizing parameters in them and is

written in Python.[66] The purpose of this work is to continue to make kinetic multilayer models codes freely available with the focus here being those which have previously been applied to multiphase indoor-relevant scientific questions. These models include K2-SURF, KM-BL, KM-FILM and KM-SUB-Skin-Clothing.[25,55,60,62,63] The α_{eff} code which simplifies the film growth part of KM-FILM is also included in this work.[26] By making these codes available, scientific research groups can apply them, adapt them to their needs and further develop them as needed to both indoor-relevant and other scientific questions.

2 Description of the models

Fig. 1 shows schematics of K2-SURF,[55] KM-BL,[60] KM-FILM,[25] the α_{eff} approach,[26] and KM-SUB-Skin-Clothing.[62,63] Detailed descriptions of the models are given in the original publications with a summary of each model and code provided below with suggestions for future potential uses and adaptations. All parameters have been labeled in the codes with a description and units and the most important parameters are also summarized in Table S1.†

2.1 K2-SURF

A schematic of the K2-SURF model which was previously used to understand measurements of reversible adsorption of limonene on an SiO_2 surface is shown in Fig. 1a.[55] Processes included in K2-SURF are adsorption and desorption to the surface and interconversion of two limonene configurations (C* up and C* down).[55] The surface accommodation coefficient of limonene on an adsorbate-free surface, the desorption lifetime, and the conversion rate coefficients between the two configurations are set to be consistent with molecular dynamics simulations.[55] Competitive adsorption is treated in the model. The effective adsorption cross-section of one limonene molecule has previously been determined by fitting to measurements and is close to the calculated geometric adsorption cross-section. The gas-phase limonene concentration is constrained to the measured limonene pressure in the reaction cell. As the pressure in the reaction cell is low, gas-phase diffusion to the surface can be ignored and is not treated in the model. The model code is included in the folder labeled 'K2-SURF' and outputs Fig. 5 from Fang *et al.*[55] which shows adsorption, equilibrium and desorption measurements and modeling of adsorbed limonene surface concentrations for three different limonene reaction cell pressures.

The model user can adapt this code to investigate any experimental systems where competitive adsorption is occurring with negligible diffusion into a bulk condensed phase. For example, we have previously adapted the code to investigate the temperature dependence of limonene surface concentrations on SiO_2 surfaces by varying the desorption lifetime of limonene

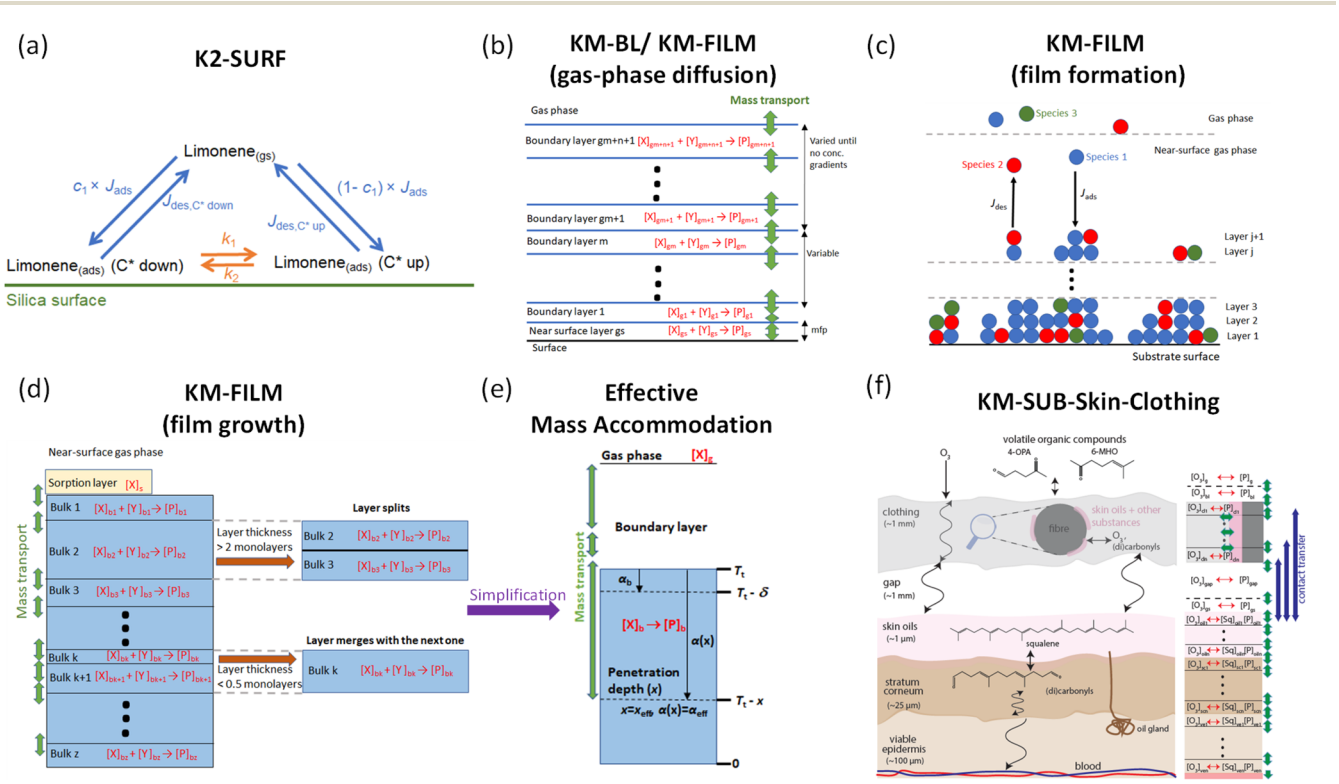

Fig. 1 Schematics of the kinetic models: (a) K2-SURF which treats the reversible adsorption of limonene to a surface,[55] (b) KM-BL which includes mass transport and chemical reactions in a boundary layer next to a surface,[60] (c) film formation through multilayer adsorption as treated in KM-FILM,[25] (d) film growth due to partitioning and mass transport of compounds as treated in KM-FILM,[25] (e) the α_{eff} approach which treats film growth in a simplified way[26] and (f) KM-SUB-Skin-Clothing which treats reactions and mass transport in the gas phase, skin and clothing.[62] This figure is based on previous publications.[25,26,55,60,62]

as a function of temperature using an Arrhenius equation.[55] Additionally, we have previously adapted the code to understand measurements of carvone reversible adsorption on a SiO_2 surface and limonene reversible adsorption on a TiO_2 surface under different relative humidities.[54,56] For this modification, two different types of desorption sites were treated ('pores' and 'non-pores') with longer desorption rates from the pore sites which could be present between the SiO_2 or TiO_2 particles used in the experiments.

2.2 KM-BL

Fig. 1b shows a schematic of the KM-BL model which was developed and described in Morrison *et al.*[60] KM-BL treats gas-phase diffusion and reactions through a boundary layer next to the surface. The boundary layer is split into layers with those closer to the surface, where significant concentration gradients may occur, being thinner than those further from the surface. Gas-phase diffusion occurs between the layers and reversible adsorption to the surface is treated from the layer closest to the surface. Fickian and turbulent diffusion in the boundary layer are included in the model.[25,60] Gas-phase reactions can also be included in the boundary layer which can reduce the effective boundary layer thickness for short-lived species as previously demonstrated for the OH radical.[60] The model currently includes three gas-phase reactions; the reaction of ozone with limonene forming OH, the reaction of OH with limonene, and a first-order loss of OH due to its reaction with other compounds. The model code is included in a folder labeled 'KM-BL' and outputs Fig. 5 from Morrison *et al.* which shows the impact of changing the O_3 uptake coefficient on the OH and O_3 concentration gradients above a surface in the presence of limonene for a relatively low turbulence intensity (K_e) of 0.1 s^{-1}.[60]

The model user can adapt this code to output the expected concentration gradients of different species above a surface, and to determine the influence of turbulence and reactions occurring in the boundary layer on the concentrations reaching a surface. This model is of particular importance for investigating how short-lived species can be rapidly formed in the boundary layer, effectively increasing their concentrations directly above the surface.[60] For example, the model could be used to better understand experimental uptake measurements of short-lived species where the flux to the surface is larger than expected.[67] A more complex reaction scheme can also be implemented flexibly. The influence of compounds which are emitted from surfaces and can react with O_3 forming OH radicals, on the OH concentration gradient in the boundary layer could also be investigated. These compounds could include lipid ozonolysis products formed from the reaction of ozone with skin oils.[16] The KM-BL model is also included in the KM-FILM model described below and can be used to investigate how boundary layer processes can impact film formation and growth.[25]

2.3 KM-FILM

The KM-FILM model consists of three parts; gas-phase diffusion through a boundary layer to the surface, film formation by multi-layer adsorption, and film growth by absorption.[25] Gas-phase diffusion through a boundary layer to the surface is treated using the KM-BL methodology described above. As shown in Fig. 1c, film formation is treated using multi-layer reversible adsorption and is an extension of K2-SURF, while being consistent with the Brunauer–Emmett–Teller (BET) theory of multi-layer adsorption.[25] The surface area of molecules and empty adsorption sites in each layer is calculated over time. Desorption rates from the first layer, which consists of molecules adsorbed to the impermeable substrate, can be set to different values from the subsequent layers. Only molecules which are uncovered by other adsorbed molecules can desorb to the gas phase. The model can also account for surface roughness by multiplying the area footprint by a roughness factor. Different compounds can reversibly adsorb at the same time. The code for film formation is in the folder labeled 'KM-FILM film formation' and outputs Fig. 2a, b, 3 and 4 from Lakey *et al.*[25] which shows examples of film formation by reproducing measurements of the mass of compounds increasing on different substrates over time.[68,69] Note that in this example the boundary layer length is set to the experimental distance between the SVOC source and the substrate. The model user should be able to apply this model to any experimental system where film formation occurs on impermeable surfaces by multi-layer adsorption.

As shown in Fig. 1d, film growth is treated using a similar approach to the KM-GAP model.[25,35] Processes included in the model are reversible adsorption, partitioning into the film and bulk diffusion. The bulk is split into several layers and the layer thickness grows and shrinks as molecules diffuse into and out of them, respectively. When the layer thickness reaches two monolayers, the layer is split into two layers; when a layer shrinks to less than half a monolayer, it merges with the next layer. This allows short diffusion lengths for accurate results and high film resolution without layers becoming unrealistically small. The code for film growth is in the folder labeled 'KM-FILM film growth' and outputs Fig. 5 from Lakey *et al.*[25] which shows film growth as a function of time due to compounds with different $\log K_{oa}$ values in the absence of bulk diffusion limitations. For this example, the boundary layer length was set to be consistent with Weschler and Nazaroff,[70] obtaining consistent results. Sensitivity tests showing the impacts of turbulence in the boundary layer, bulk diffusion limitations and reactions have previously been performed and are shown in Lakey *et al.*[25] The model has also previously been adapted to investigate surfaces acting as reservoirs, where compounds can rapidly partition into a surface film and are then released back into the gas-phase over a prolonged period of time.[26] The model user could perform similar sensitivity tests or apply the model to their own experimental or theoretical system to investigate film growth or surfaces acting as reservoirs.

2.4 Effective mass accommodation equation

Fig. 1e shows a schematic of the model with the effective mass accommodation coefficient (α_{eff}).[26] The α_{eff} is defined in eqn

(E1) and is the probability that a molecule that collides with a surface will be taken up into the bulk with effective penetration depth (x_{eff}) while accounting for the surface mass accommodation coefficient (α_s), partitioning coefficient (K_{oa}), bulk diffusion coefficient (D_b), and chemical reactions.[26,61]

$$\alpha_{eff} = \alpha_s \frac{1}{1 + \frac{\alpha_s \omega x_{eff}}{4 D_b K_{oa}}} \quad \text{(E1)}$$

where ω is the mean thermal velocity and x_{eff} is the effective penetration depth which is equal to a third of the total film thickness (T_t) in the absence of reactions:[26]

$$x_{eff} = \frac{T_t}{3} \quad \text{(E2)}$$

In the presence of reactions the penetration length should be changed as defined in our previous publication and shown below:[26]

$$x_{eff} = T_t \left(\frac{1 - Q}{q \tanh(q)} \right) \quad \text{(E3)}$$

where $Q = \tanh(q)/q$ and $q = T_t(k_{br}/D_b)$. k_{br} is the first-order reaction rate coefficient and D_b is the bulk diffusion coefficient. The α_{eff} equation simplifies the film growth part of KM-FILM and can output similar results under many scenarios. The main advantage of using α_{eff} is that it is easy to implement in indoor air models to account for bulk diffusion limitations, and it is much less computationally expensive to run than KM-FILM. However, it should be noted that it can only treat first-order bulk reactions and may output results which differ from KM-FILM before quasi-steady-state has been reached in the penetration depth. The bulk accommodation coefficient (α_b) which is the probability that a molecule colliding with a surface will enter the near-surface bulk should be used rather than the α_{eff} whenever $\alpha_b < \alpha_{eff}$.

The equation has been incorporated into a model code that is included in the folder labeled 'effective mass accommodation' and outputs Fig. 3b from Lakey *et al.*[26] which shows total film thickness after partitioning of compounds with different $\log K_{oa}$ values into a film as a function of the bulk diffusion coefficient. We have previously adapted this code to investigate the potential impact of chemical reactions on film growth and the ability of surfaces to act as reservoirs for compounds with different $\log K_{oa}$ values, bulk diffusion coefficients and for different film thicknesses.[26] The code can be further adapted by the user to investigate these effects, while α_{eff} can be included in indoor air models to account for reduced uptake to viscous surfaces.

2.5 KM-SUB-Skin-Clothing

Fig. 1f shows a schematic of the KM-SUB-Skin-Clothing model.[62] The model includes a gas phase, boundary layer, clothing, gap between the clothing and the skin, skin oil, stratum corneum, viable epidermis and blood vessels. The clothing, skin oil, stratum corneum and viable epidermis have been split into several layers to maintain short diffusion distances. Mass transport occurs between layers. In the clothing, diffusion is effectively slowed down by partitioning into skin oils and other substances which are present on clothing fibers. The model treats contact transfer of skin oil between the top layer of the skin and the clothing. Chemical reactions occur in both the gas phase and clothing and skin. Two model codes have been included. The original model code is included in the folder 'KM-SUB-Skin-Clothing' and is set up to output the time evolution of ozone and gas-phase squalene ozonolysis products when two people enter a room (Fig. 6a in Lakey *et al.*).[62] Parameters are set to be consistent with the measurements from Wisthaler and Weschler (2010) and reproduce their measurements well.[14] In this version of the code the chemistry has been simplified and only carbonyl products are formed and a 100% yield is assumed. The second model code is included in the folder 'KM-SUB-Skin-Clothing RH' and is also set up to be consistent with Wisthaler and Weschler (2010).[14,63] The second model code is updated by having a more complex chemical mechanism where Criegee intermediates and subsequent reactions are treated. This model code is set up to output the change in the concentrations of different squalene ozonolysis products as a function of relative humidity (solid lines in Fig. 6 of Lakey *et al.*).[63]

The model user can adapt these codes to investigate reactions between oxidants and lipids in skin and clothing. Model parameters can be changed to experimental conditions. The mechanism can be changed as required depending on the products being investigated and the model complexity and accuracy that the user requires. For example, we have previously updated the mechanism to include the formation of OH radicals in the gas phase and calculated OH reactivity to compare it to measurements.[16] We have also previously adapted the code to reproduce measurements performed on soiled clothing in the absence of people.[62] This can be done by removing the skin specific layers and processes from the model. The code can also be adapted to model human skin in the absence of clothing by removing clothing-specific layers and processes.[62] The resulting model should be similar to our KM-SUB-Skin model but with the inclusion of a boundary layer next to the skin which was not included in that model.[71]

3 Running the models

All models can be run using MATLAB R2023b which can be downloaded from the MathWorks website. Once the model files have been opened, the 'Current Folder' in MATLAB must be changed to match the one containing the files. The models can then be run by viewing the script containing the solver (*i.e.* not the one containing the differential equations that ends in _F) and pressing the 'Run' button on the Editor tab. The models will calculate and output either the concentration or the number of molecules for each compound in each layer. After the model has been run, the outputs can be found in the 'Workspace'. One of the major considerations and potential limitations when running the models is the computational time that they require. Fig. S1† summarizes the typical computational times that the different models take to run, which vary from less than a second to more than a day. Computational time increases significantly

as the number of layers or number of reactions in the model increases. These times are also likely to be affected by the processor used and can also be affected by the type and number of other programs running on the computer at the same time.

There are several technical points which should be noted before running the models to obtain accurate results. The models use either the ode23tb or ode23s solvers to perform calculations and output results. The ode23tb solver is usually adequate and runs significantly faster than the ode23s solver but may occasionally produce slightly less accurate results for stiff calculations and it is therefore important to choose the solver carefully. When using the KM-BL and KM-SUB-Skin-Clothing codes, the number of layers must be large enough to obtain convergence so that the outputs are accurate. This can be tested by running the model with increasing numbers of layers until the output does not change. Similarly, for the film formation part of KM-FILM, the user must set the number of potential adsorption layers at the start of the simulation to a large enough number so that the results of the simulation are not impacted. The number of potential adsorption layers is set to 101 for outputting the results in Lakey *et al.*,[25] but may need to be increased if parameters such as gas-phase concentrations, desorption lifetimes or experimental times increase. For the film growth part of KM-FILM, the thickness at which a layer splits or merges can be increased if the simulation is too computationally expensive, but the user should ensure that the layers do not become so thick that this impacts the model outputs. If the boundary layer thickness in KM-BL has not been specified, the user should test that the total boundary layer length is thick enough that the concentration of species at the furthest distances from the surface are constant. Although excellent agreement has been obtained between the KM-FILM model and the α_{eff} approach for many scenarios, the user should always be aware that deviations may occur if quasi-equilibrium has not been obtained in the penetration depth.[26] The user may be able to reduce the discrepancy by decreasing and continuously updating the penetration depth to the distance that a molecule will have travelled at a given time $(D_b t)^{0.5}$ as previously discussed, but this should be further validated using KM-FILM.[26]

The models can be adapted and changed as required, for example, by adding additional reactions, processes, species, or outputs. Parameters such as the initial concentrations should be changed to reflect the experimental or hypothetical scenario being investigated. Other parameters such as gas-phase diffusion coefficients, partitioning coefficients, bulk diffusion coefficients, surface mass accommodation coefficients, desorption rate coefficients or reaction rate coefficients could be estimated from published values and equations in the literature or molecular dynamic (MD) simulations.[72–78] If only a few parameters exist, it is often possible to vary the values systematically within a sensible range until the measurements can be reproduced. Alternatively, the model can be coupled with a code which automatically varies parameters until the data has been fitted. For example, we have previously used the Monte Carlo Genetic Algorithm (MCGA) to determine unknown and uncertain parameters.[79] This code runs the model with many different parameter sets and assigns a fitting value to each one. The parameter sets are then combined using processes such as survival, recombination, and mutation to improve the fitting values. The MCGA can also be run multiple times to check the uncertainty in parameters, whether there are several parameter sets that exist which can fit the data well, and whether any codependences may exist between parameters (*i.e.* where the same fitting is obtained when two or more parameters are changed in a systematic way).[36,42,57,79,80] Note that Monte Carlo codes are freely available online on the MATLAB website and there are many other ways of optimizing parameters. It is also important to note that by fitting parameters in the models to many different experimental data sets, obtained under a wide range of conditions, parameters become significantly more constrained. This increases our confidence in using the model to extrapolate to new scenarios. However, some parameters may still not be constrained accurately such as in KM-SUB-Skin-Clothing where natural variability in people and clothing can impact results and sensitivity tests should be performed using a range of values for uncertain parameters.

4 Model outputs

Fig. 2 and 3 show examples of outputs from the different models and focus on the impact of changing specific parameters on model outputs. All results have been obtained by changing the parameter of interest in the model codes attached to this publication and should help the model user familiarize themselves with important processes included in the model. Fig. 2a shows the effect of changing the limonene desorption lifetime on the limonene equilibrium surface concentration for three different gas-phase limonene pressures which were investigated in Fang *et al.* (2019).[55] As the desorption lifetime decreases, limonene molecules desorb from the surface at a faster rate leading to lower limonene surface concentrations. At higher limonene desorption lifetimes, the adsorption sites become full, resulting in the surface concentrations no longer being as dependent on the limonene pressure.

Fig. 2b shows the impact of changing K_e and the first-order rate coefficient for the background loss of OH ($k_{gr,OH}$) on the OH concentration gradient above the surface. O_3 reacts with limonene in the boundary layer forming OH radicals which are subsequently lost by reaction with limonene and other species. The O_3 uptake coefficient to the surface is set to be 5×10^{-4}, which is a typical value for O_3 uptake to skin oils, while the OH uptake coefficient is set to be 1 reflecting its high reactivity.[81] With higher $k_{gr,OH}$ the bulk gas-phase concentration (*i.e.* beyond the boundary layer) of OH is lower. With more turbulence, the diffusion rate of O_3 through the boundary layer increases leading to higher O_3 concentrations right above the surface, resulting in higher production rates and concentrations of OH. Interestingly, by directly comparing a scenario with high turbulence and high OH background loss ($K_e = 10\ s^{-1}$ and $k_{gr,OH} = 50\ s^{-1}$) to a scenario with low turbulence and low OH background loss ($K_e = 0.1\ s^{-1}$ and $k_{gr,OH} = 1\ s^{-1}$) we demonstrate that even with lower OH gas-phase concentrations, greater

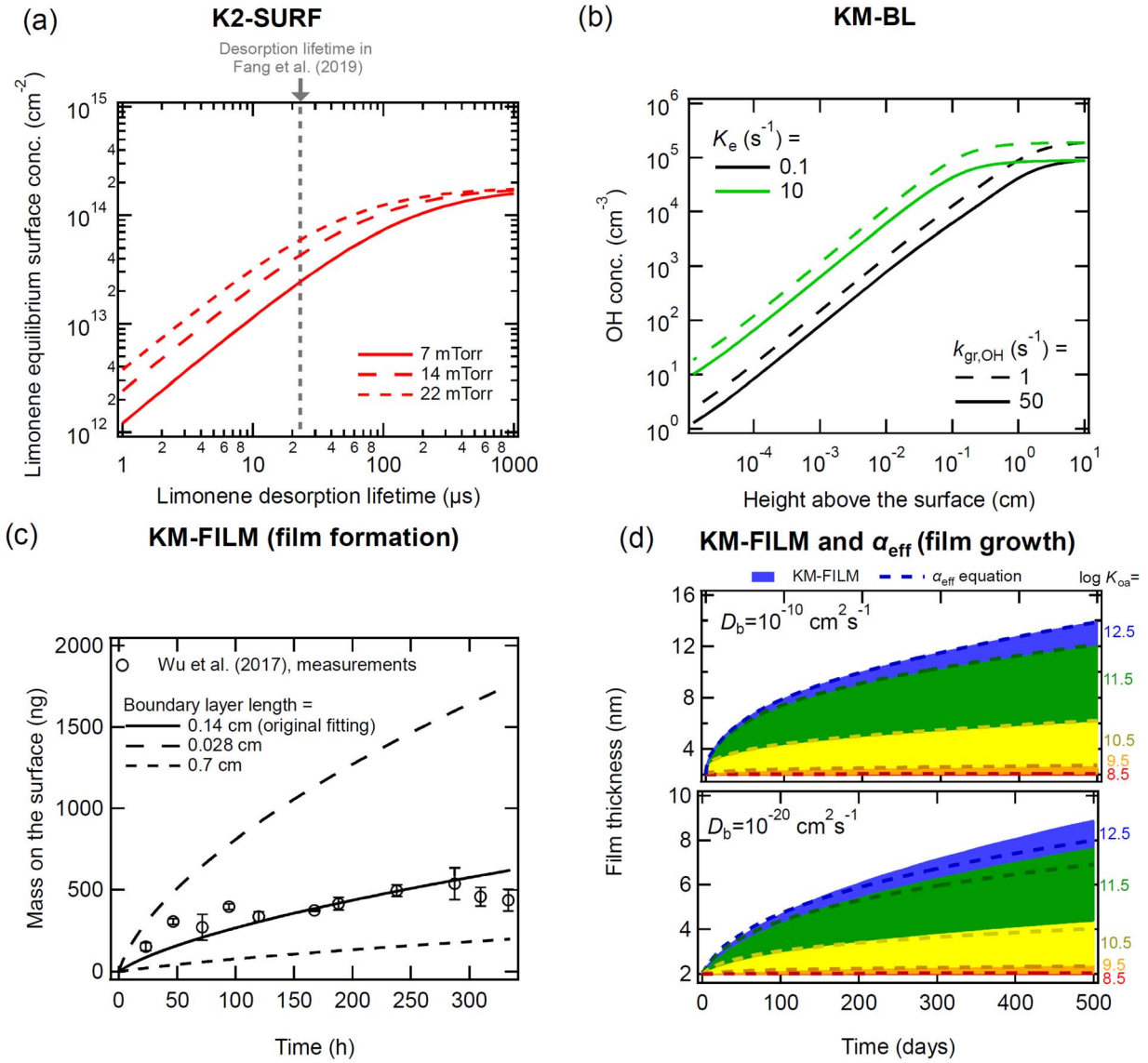

Fig. 2 Exemplary simulations of kinetic models to investigate the impact of (a) limonene desorption lifetimes on limonene surface concentrations using the K2-SURF model,[55] (b) the turbulence intensity and the background OH decay rate coefficient on the OH concentration gradient in the boundary layer with an ozone uptake coefficient of 5×10^{-4} using the KM-BL model and with $K_e = 0.1$ (black) and 10 (green) and $k_{b,OH} = 1$ (dashed) and 50 (solid),[60] (c) the boundary layer length on surface film growth using the KM-FILM model[25] and (d) the bulk diffusion coefficient on film growth due to compounds with different log K_{oa} values using the KM-FILM model[28] and the α_{eff} equation.[26] All figures are produced using the set up described in the 'Description of the models' section and with only the parameters shown in the panels being varied.

turbulence in the boundary layer can cause OH concentrations right above the surface to be higher (Fig. 2b).

Fig. 2c shows measurements and modeling of mass accumulation of di-2-ethylhexyl phthalate (DEHP) on an aluminum surface due to multi-layer adsorption and the impact of changing the boundary layer length. The original fitting and parameters are provided in Lakey *et al.* (2021)[25] and the original boundary layer length is set to 0.14 cm which is the distance between the SVOC source and the aluminum surface in the experiments.[82] Additional lines show the impact of increasing or reducing the boundary layer length by a factor of 4. As the boundary layer length increases, gas-phase diffusion limitations increase, leading to lower gas-phase concentrations right above the surface, resulting in less adsorption and a lower surface mass. This demonstrates the importance of the diffusion gap length between the SVOC source and test material on the amount of phthalate to be adsorbed to a test material. It is also worth noting that by assuming a typical deposition velocity of 3 m h^{-1} (0.083 cm s^{-1}) to indoor surfaces and a gas-phase diffusion coefficient of 0.06 cm^2 s^{-1}, the boundary layer length in a room is likely to be approximately 0.7 cm, leading to a larger gas-phase diffusion limitation than in the original experiments.[2] Turbulence is also extremely important as it can reduce the boundary layer length leading to an increase in the amount of mass being deposited to a surface.[60]

Fig. 2d shows film growth as a function of time due to the partitioning of compounds with different log K_{oa} values with film phase state being low viscous liquid with bulk diffusion

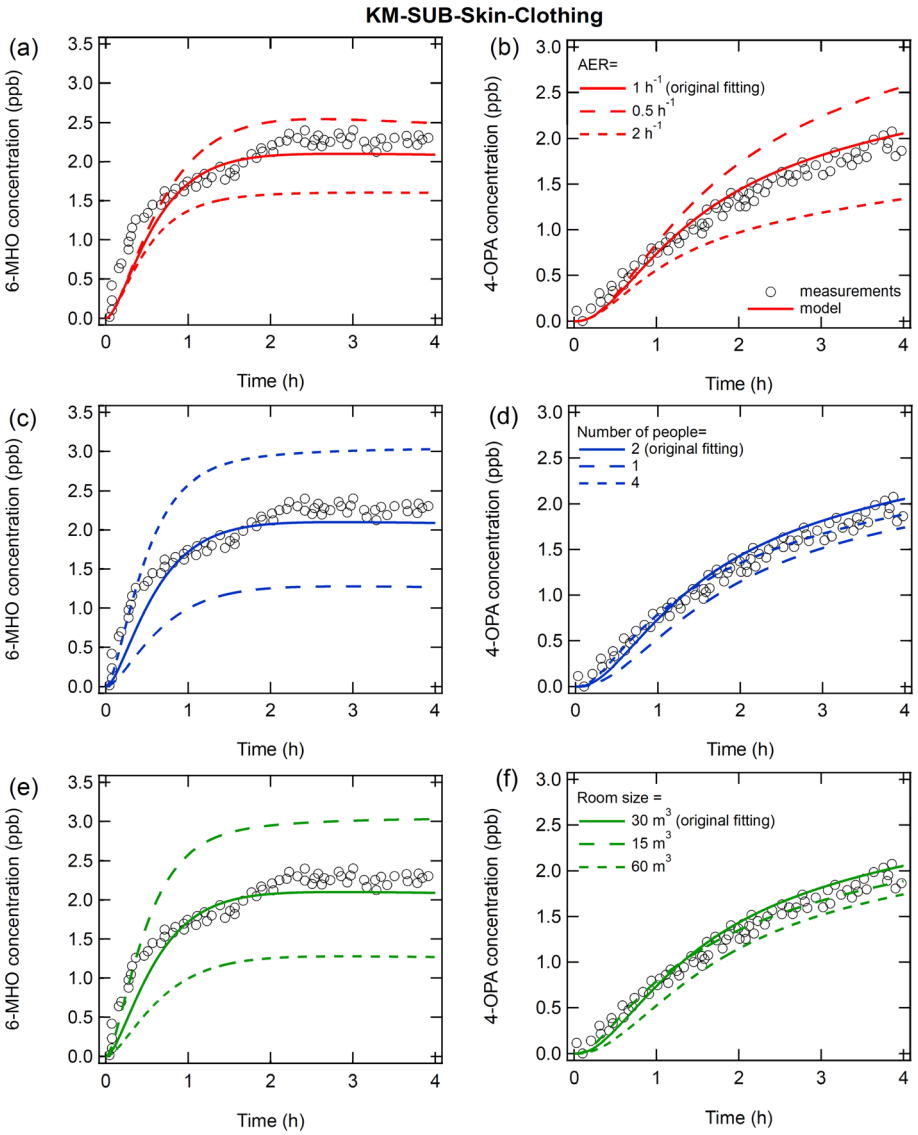

Fig. 3 Mixing ratios of 6-MHO and 4-OPA as simulated by the KM-SUB-Skin-Clothing model with the simplified reaction mechanism. Measurements are from Wisthaler and Weschler (2010)[14] and model parameters can be found in Lakey *et al.*[62] Sensitivity tests were performed to investigate the impact of (a and b) air-exchange rate, (c and d) the number of people and (e and f) the room size on the gas-phase concentration of (a, c and e) 6-MHO and (b, d and f) 4-OPA.

coefficients (D_b) of 10^{-10} cm^2 s^{-1} and being highly viscous (semi-)solid with D_b of 10^{-20} cm^2 s^{-1}. The film growth results for $D_b = 10^{-10}$ cm^2 s^{-1} are consistent with previous work where bulk diffusion limitations are negligible.[25,70] The KM-FILM model and α_{eff} equation agree well. When D_b is decreased to 10^{-20} cm^2 s^{-1}, bulk diffusion limitations become important, causing the film to grow at a slower rate and significantly reducing the total thickness after 500 days (~9 nm compared to ~14 nm). There are small deviations between the film thicknesses outputted by the KM-FILM model and the α_{eff} equation which are due to equilibrium taking longer to be established in the penetration depth for smaller diffusion coefficients. The differences are also enhanced by less overall partitioning occurring into the slightly thinner films outputted by the α_{eff} equation.

Fig. 3 shows the gas-phase concentrations of two squalene ozonolysis products, 6-MHO (monocarbonyl, primary product) and 4-OPA (dicarbonyl, secondary product) as a function of air exchange rate, number of people in the room and room size. The original fittings to the data and parameters are provided in previous publications[62,71] and the effect of these parameters have previously been investigated using the KM-SUB-Skin model with similar trends being observed. For clarity, Fig. 3 only shows results from the original KM-SUB-Skin-Clothing model. For comparison purposes, Fig. S2† shows these same results as well as outputs from the model with the more complex mechanism involving Criegee intermediates. The trends outputted by the two model versions are the same and differences between the results of the two models are mainly caused by variations in the fitting of the original experimental data.

Fig. 3a and b show that, as air exchange increases, molecules are removed by indoor-to-outdoor transport at a faster rate leading to lower indoor gas-phase concentrations. The absolute concentrations of these products are also impacted by ozone concentrations which will increase as outdoor-to-indoor transport increases. Fig. 3c and d demonstrate that as the number of people in a room increases the concentration of 6-MHO increases, while changes in 4-OPA concentrations are small. Increasing the number of people leads to a greater skin and clothing surface area in the room, resulting in more squalene reacting with ozone and an increased formation of primary products such as 6-MHO as well as a decrease in ozone concentrations. Secondary products such as 4-OPA are formed from primary products reacting with ozone. The overall effect of the changes in primary product and ozone concentrations causes only small changes in 4-OPA concentrations over the range of people investigated here. Fig. 3e and f shows the impact of room size on the gas-phase concentrations of 6-MHO and 4-OPA. As the room size increases, primary products become diluted leading to lower gas-phase concentrations. However, ozone concentrations in the room increase with increasing room size as the surface area of people to the volume of the room decreases. The 4-OPA concentration is impacted by dilution as well as the concentrations of primary products and ozone resulting in only small changes over the room sizes that are investigated here.

5 Connections to other indoor models

The connection between different types of indoor models was originally discussed in the modelling consortium for chemistry in indoor environments (MOCCIE) overview paper.[31] Below we will discuss specific recent examples of how our multilayer kinetic models have connected with other indoor models as well as the potential for future connections.

MD simulations can estimate many fundamental parameters that are used as inputs to kinetic multilayer models such as surface accommodation coefficients (α_s), desorption lifetimes (τ_d), partitioning coefficients (K), and bulk diffusion coefficients (D_b). MD simulations have determined these parameters for ozone and important squalene ozonolysis products interacting with skin oil.[62,73] A range of sensitivity tests using KM-SUB-Skin-Clothing indicated that gas-phase concentrations of ozone and the carbonyl products were insensitive to the changes in α_s, τ_d and D_b, but were significantly impacted by changing K, which were subsequently updated in the next version of KM-SUB-Skin-Clothing.[63,73] The KM-SUB-Skin-Clothing and MD simulations were cross-validated by outputting the bulk accommodation coefficients, yielding consistent results.[73] Additional parameters, such as D_b in the stratum corneum which is a very sensitive parameter, could be updated in KM-SUB-Skin-Clothing in the future as MD simulation results become available.

MD simulations have also been used to constrain α_s, τ_d, K and D_b of ozone for triolein films in the KM-GAP model and experimental measurements were reproduced well.[59] MD simulations of α_s and τ_d for limonene on SiO_2 surfaces were used to constrain these parameters in K2-SURF and good agreement with measurements were obtained.[55] The adsorption enthalpy estimated from K2-SURF was also in agreement with the value obtained from MD simulations.[55] In contrast, initial K2-SURF simulations of carvone adsorbing on SiO_2 with α_s and τ_d values constrained by MD simulations, were not able to reproduce the rapid adsorption and slow desorption kinetics observed in experiments.[54] This indicated that there was likely to be a missing process in K2-SURF, which was speculated to be the trapping of molecules in pores retarding the desorption. By including this process, measurements were able to be reproduced using K2-SURF while maintaining consistency with MD simulations.[54] Overall, MD simulations are very useful to constrain parameters for a wide range of different indoor surfaces and compounds, reducing uncertainties in kinetic multiphase models.

Kinetic multilayer models assume a well-mixed gas phase indoors, while computational fluid dynamics (CFD) simulations resolve indoor air flow to simulate spatial distributions of indoor air constituents.[83] Spatial gradients can have consequences with regards to human exposure and may also impact the validity of indoor measurements which are usually only performed in one position. Kinetic multilayer models can be used to output near surface concentrations, yields and uptake coefficients of compounds which can be used as inputs to CFD models. By performing a range of sensitivity tests, the kinetic multilayer models can also determine the most important gas-phase reactions which can also be implemented in CFD models. The KM-SUB-Skin-Clothing model has been used to generate inputs to CFD simulations for several studies.[16,62,64] The CFD simulations have concluded that primary squalene ozonolysis products will be more concentrated near soiled clothing and in the breathing zone compared to the room air, while secondary ozonolysis products are more evenly distributed.[64] Additionally, OH reactivity is elevated close to the human body and OH concentrations are depleted which may have consequences with regards to the oxidation level of compounds reaching the breathing zone through the thermal plume around the human body.[16] In the future, the combination of the KM-SUB-Skin-Clothing model with the CFD model could be used to investigate the spatial distribution of additional compounds as a function of relative humidity and the impact of using fragrances and lotions. Adaptations to the codes could enable spatial distributions of particles, formed from the reaction of ozone with skin oils, to be investigated.[84–86] The CFD model could also be combined with other indoor multilayer models, such as KM-FILM. A kinetic box model has also been combined with CFD simulations to estimate the spatial distribution and temporal evolution of bleach products and general equations for estimating whether spatial concentration gradients are expected are presented in that study.[83]

Currently, indoor chemistry models such as the Indoor CHEMical model in Python (INCHEM-Py) and the Indoor Model of Aerosols, Gases, Emissions, and Surfaces (IMAGES) do not explicitly treat the impact of surface film viscosity on surface deposition.[87–89] While the KM-FILM model would be too

computationally expensive to couple with these models, the effective mass accommodation equation can easily be implemented. By including this equation, the potential effect of film viscosity on indoor chemical compound concentrations can be investigated for a range of scenarios. A similar equation that was developed for partitioning into particles of different viscosities has already been successfully implemented in IMAGES,[30,61] demonstrating that gas-particle partitioning can be retarded due to diffusion limitations.[30]

6 Summary and future developments

In this study, the annotated codes for kinetic multilayer models for indoor multiphase adsorption, partitioning, diffusion and chemistry are made publicly available. These codes allow the temporal evolution of compound concentrations in different phases to be determined and can explicitly treat bulk concentration gradients. They use fundamental parameters such as the surface accommodation coefficient (α_s), desorption lifetime (τ_d), bulk diffusion coefficient (D_b), gas-phase diffusion coefficient (D_g), bulk and surface reaction rate coefficients (k_{br} and k_{sr}), and partitioning coefficients (K) which can be determined from literature values, MD simulations or from fitting to experimental measurements. The KM-SUB-Skin-Clothing model treats the ozonolysis of skin lipids and their products, the K2-SURF model treats reversible adsorption from indoor relevant surfaces, the KM-BL model treats mass transport and reactions in the boundary layer, and the KM-FILM codes treat film formation and growth. The code for the α_{eff} equation is also published in this work to effectively treat film growth.

The published codes have a wide range of possible future uses and can be further developed as follows. By making these codes publicly available, scientific research groups can apply them to a range of multiphase laboratory experiments and indoor field campaigns to test hypotheses and subsequently extrapolate to different conditions. The codes can be used to identify the rate-limiting processes and reactions. Codes can be adapted as required to reflect experimental conditions and the user can also change, add, or remove compounds, reactions, and outputs as required. Near-surface concentrations, yields and uptake coefficients have previously been outputted and can be used as inputs to CFD simulations to investigate spatial distributions. The α_{eff} equation can be included in indoor models to reflect the impact of surface viscosity on surface deposition.

Further developments of the model may be able to address important research questions and more accurately represent indoor multiphase chemistry. For example, the film thickness at which absorption can occur and becomes more important than adsorption remains unclear and could be investigated and included in KM-FILM when relevant experimental measurements become available. Chemical reactions and species have been generalized in KM-FILM and future developments could treat specific classes of chemical compounds and the specific reactions that they can undergo in indoor surfaces. Models could also be set up to include different types of surface in a single indoor space (*e.g.* with different viscosities) to investigate how partitioning into one surface type would influence partitioning into a different type of surface. Additionally, the ozonolysis of skin lipids on non-human indoor surfaces can be treated in future studies as measurements have indicated that off-body skin lipids have a large influence on indoor ozone chemistry.[90] Reversible partitioning of lipid ozonolysis products into non-human indoor surfaces could also be included in the future. The code could also be adapted to include the nucleation and formation of nanocluster particles.[84–86] Additionally, the impact of personal care products such as fragrances and lotions could be investigated.

Data availability

All model codes and data are available in the ESI.†

Conflicts of interest

There are no conflicts to declare.

Acknowledgements

This work was funded by the Alfred P. Sloan Foundation (G-2020-13912). We thank our collaborators contributing to the development of these models.

References

1 A. Manuja, J. Ritchie, K. Buch, Y. Wu, C. M. Eichler, J. C. Little and L. C. Marr, Total surface area in indoor environments, *Environ. Sci.: Processes Impacts*, 2019, **21**, 1384–1392.
2 C. J. Weschler and W. W. Nazaroff, Semivolatile organic compounds in indoor environments, *Atmos. Environ.*, 2008, **42**, 9018–9040.
3 W. D. Fahy, F. Wania and J. P. Abbatt, When Does Multiphase Chemistry Influence Indoor Chemical Fate?, *Environ. Sci. Technol.*, 2024, **58**, 4257–4267.
4 C. Wang, D. B. Collins, C. Arata, A. H. Goldstein, J. M. Mattila, D. K. Farmer, L. Ampollini, P. F. DeCarlo, A. Novoselac and M. E. Vance, Surface reservoirs dominate dynamic gas-surface partitioning of many indoor air constituents, *Sci. Adv.*, 2020, **6**, eaay8973.
5 A. H. Goldstein, W. W. Nazaroff, C. J. Weschler and J. Williams, How do indoor environments affect air pollution exposure?, *Environ. Sci. Technol.*, 2020, **55**, 100–108.
6 J. P. Abbatt and C. Wang, The atmospheric chemistry of indoor environments, *Environ. Sci.: Processes Impacts*, 2020, **22**, 25–48.
7 W. W. Nazaroff and C. J. Weschler, Indoor ozone: Concentrations and influencing factors, *Indoor Air*, 2022, **32**, e12942.
8 E. Harding-Smith, H. L. Davies, C. O'Leary, R. Winkless, M. Shaw, T. Dillon, B. Jones and N. Carslaw, The impact of surfaces on indoor air chemistry following cooking and

cleaning, *Environ. Sci.: Processes Impacts*, 2024, DOI: 10.1039/D4EM00410H.

9 C. Y. Lim and J. P. Abbatt, Chemical Composition, Spatial Homogeneity, and Growth of Indoor Surface Films, *Environ. Sci. Technol.*, 2020, **54**, 14372–14379.

10 B. L. Deming and P. J. Ziemann, Quantification of alkenes on indoor surfaces and implications for chemical sources and sinks, *Indoor Air*, 2020, **30**, 914–924.

11 V. W. Or, M. Wade, S. Patel, M. R. Alves, D. Kim, S. Schwab, H. Przelomski, R. O'Brien, D. Rim and R. L. Corsi, Glass surface evolution following gas adsorption and particle deposition from indoor cooking events as probed by microspectroscopic analysis, *Environ. Sci.: Processes Impacts*, 2020, **22**, 1698–1709.

12 V. W. Or, M. R. Alves, M. Wade, S. Schwab, R. L. Corsi and V. H. Grassian, Crystal clear? Microspectroscopic imaging and physicochemical characterization of indoor depositions on window glass, *Environ. Sci. Technol. Lett.*, 2018, **5**, 514–519.

13 D. K. Farmer, M. E. Vance, J. P. Abbatt, A. Abeleira, M. R. Alves, C. Arata, E. Boedicker, S. Bourne, F. Cardoso-Saldaña and R. Corsi, Overview of HOMEChem: House observations of microbial and environmental chemistry, *Environ. Sci.: Processes Impacts*, 2019, **21**, 1280–1300.

14 A. Wisthaler and C. J. Weschler, Reactions of ozone with human skin lipids: Sources of carbonyls, dicarbonyls, and hydroxycarbonyls in indoor air, *Proc. Natl. Acad. Sci. U.S.A.*, 2010, **107**, 6568–6575.

15 B. Coffaro and C. P. Weisel, Reactions and Products of Squalene and Ozone: A Review, *Environ. Sci. Technol.*, 2022, **56**, 7396–7411.

16 N. Zannoni, P. S. J. Lakey, Y. Won, M. Shiraiwa, D. Rim, C. J. Weschler, N. Wang, L. Ernle, M. Li, G. Bekö, P. Wargocki and J. Williams, The human oxidation field, *Science*, 2022, **377**, 1071–1077.

17 A. P. Ault, V. H. Grassian, N. Carslaw, D. B. Collins, H. Destaillats, D. J. Donaldson, D. K. Farmer, J. L. Jimenez, V. F. McNeill and G. C. Morrison, Indoor Surface Chemistry: Developing a Molecular Picture of Reactions on Indoor Interfaces, *Chem*, 2020, **6**, 3203–3218.

18 B. C. Singer, A. T. Hodgson, T. Hotchi, K. Y. Ming, R. G. Sextro, E. E. Wood and N. J. Brown, Sorption of organic gases in residential rooms, *Atmos. Environ.*, 2007, **41**, 3251–3265.

19 K. Kristensen, D. M. Lunderberg, Y. Liu, P. K. Misztal, Y. Tian, C. Arata, W. W. Nazaroff and A. H. Goldstein, Sources and dynamics of semivolatile organic compounds in a single-family residence in northern California, *Indoor Air*, 2019, **29**, 645–655.

20 D. B. Collins, R. F. Hems, S. Zhou, C. Wang, E. Grignon, M. Alavy, J. A. Siegel and J. P. Abbatt, Evidence for gas–surface equilibrium control of indoor nitrous acid, *Environ. Sci. Technol.*, 2018, **52**, 12419–12427.

21 R. Sheu, C. F. Fortenberry, M. J. Walker, A. Eftekhari, C. Stönner, A. Bakker, J. Peccia, J. Williams, G. C. Morrison and B. J. Williams, Evaluating Indoor Air Chemical Diversity, Indoor-to-Outdoor Emissions, and Surface Reservoirs Using High-Resolution Mass Spectrometry, *Environ. Sci. Technol.*, 2021, **55**, 10255–10267.

22 D. M. Lunderberg, K. Kristensen, Y. Tian, C. Arata, P. K. Misztal, Y. Liu, N. Kreisberg, E. F. Katz, P. F. DeCarlo and S. Patel, Surface emissions modulate indoor SVOC concentrations through volatility-dependent partitioning, *Environ. Sci. Technol.*, 2020, **54**, 6751–6760.

23 J. Li, M. F. Link, S. Pandit, M. H. Webb, K. J. Mayer, L. A. Garofalo, K. L. Rediger, D. G. Poppendieck, S. M. Zimmerman, M. E. Vance, V. H. Grassian, G. C. Morrison, B. J. Turpin and D. K. Farmer, The persistence of smoke VOCs indoors: Partitioning, surface cleaning, and air cleaning in a smoke-contaminated house, *Sci. Adv.*, 2023, **9**, eadh8263.

24 S. Wu, S. K. Hayati, E. Kim, A. P. de la Mata, J. J. Harynuk, C. Wang and R. Zhao, Henry's Law Constants and Indoor Partitioning of Microbial Volatile Organic Compounds, *Environ. Sci. Technol.*, 2022, **56**, 7143–7152.

25 P. S. Lakey, C. M. Eichler, C. Wang, J. C. Little and M. Shiraiwa, Kinetic multi-layer model of film formation, growth, and chemistry (KM-FILM): Boundary layer processes, multi-layer adsorption, bulk diffusion, and heterogeneous reactions, *Indoor Air*, 2021, **31**, 2070–2083.

26 P. S. Lakey, B. E. Cummings, M. S. Waring, G. C. Morrison and M. Shiraiwa, Effective mass accommodation for partitioning of organic compounds into surface films with different viscosities, *Environ. Sci.: Processes Impacts*, 2023, **25**, 1464–1478.

27 R. E. O'Brien, Y. Li, K. J. Kiland, E. F. Katz, V. W. Or, E. Legaard, E. Q. Walhout, C. Thrasher, V. H. Grassian and P. F. DeCarlo, Chemical and physical properties of organic mixtures on indoor surfaces during HOMEChem, *Environ. Sci.: Processes Impacts*, 2021, **23**, 559–568.

28 S. Xu, F. Mahrt, F. K. Gregson and A. K. Bertram, Possible Effects of Ozone Chemistry on the Phase Behavior of Skin Oil and Cooking Oil Films and Particles Indoors, *ACS Earth Space Chem.*, 2022, **6**, 1836–1845.

29 B. E. Cummings, Y. Li, P. F. DeCarlo, M. Shiraiwa and M. S. Waring, Indoor aerosol water content and phase state in US residences: impacts of relative humidity, aerosol mass and composition, and mechanical system operation, *Environ. Sci.: Processes Impacts*, 2020, **22**, 2031–2057.

30 B. E. Cummings, M. Shiraiwa and M. S. Waring, Phase state of organic aerosols may limit temperature-driven thermodynamic repartitioning following outdoor-to-indoor transport, *Environ. Sci.: Processes Impacts*, 2022, **24**, 1678–1696.

31 M. Shiraiwa, N. Carslaw, D. J. Tobias, M. S. Waring, D. Rim, G. Morrison, P. S. Lakey, M. Kruza, M. Von Domaros and B. E. Cummings, Modelling consortium for chemistry of indoor environments (MOCCIE): integrating chemical processes from molecular to room scales, *Environ. Sci.: Processes Impacts*, 2019, **21**, 1240–1254.

32 U. Pöschl, Y. Rudich and M. Ammann, Kinetic model framework for aerosol and cloud surface chemistry and gas-particle interactions - Part 1: General equations,

parameters, and terminology, *Atmos. Chem. Phys.*, 2007, **7**, 5989–6023.

33 M. Shiraiwa, R. M. Garland and U. Pöschl, Kinetic double-layer model of aerosol surface chemistry and gas-particle interactions (K2-SURF): Degradation of polycyclic aromatic hydrocarbons exposed to O_3, NO_2, H_2O, OH and NO_3, *Atmos. Chem. Phys.*, 2009, **9**, 9571–9586.

34 M. Shiraiwa, C. Pfrang and U. Pöschl, Kinetic multi-layer model of aerosol surface and bulk chemistry (KM-SUB): the influence of interfacial transport and bulk diffusion on the oxidation of oleic acid by ozone, *Atmos. Chem. Phys.*, 2010, **10**, 3673–3691.

35 M. Shiraiwa, C. Pfrang, T. Koop and U. Poeschl, Kinetic multi-layer model of gas-particle interactions in aerosols and clouds (KM-GAP): linking condensation, evaporation and chemical reactions of organics, oxidants and water, *Atmos. Chem. Phys.*, 2012, **12**, 2777–2794.

36 T. Berkemeier, S. S. Steimer, U. K. Krieger, T. Peter, U. Poschl, M. Ammann and M. Shiraiwa, Ozone uptake on glassy, semi-solid and liquid organic matter and the role of reactive oxygen intermediates in atmospheric aerosol chemistry, *Phys. Chem. Chem. Phys.*, 2016, **18**, 12662–12674.

37 P. Davidovits, C. E. Kolb, L. R. Williams, J. T. Jayne and D. R. Worsnop, Mass accommodation and chemical reactions at gas– liquid interfaces, *Chem. Rev.*, 2006, **106**, 1323–1354.

38 D. R. Worsnop, J. W. Morris, Q. Shi, P. Davidovits and C. E. Kolb, A chemical kinetic model for reactive transformations of aerosol particles, *Geophys. Res. Lett.*, 2002, **29**, 57.

39 T. Berkemeier, A. J. Huisman, M. Ammann, M. Shiraiwa, T. Koop and U. Pöschl, Kinetic regimes and limiting cases of gas uptake and heterogeneous reactions in atmospheric aerosols and clouds: a general classification scheme, *Atmos. Chem. Phys.*, 2013, **13**, 6663–6686.

40 T. Berkemeier, M. Shiraiwa, U. Pöschl and T. Koop, Competition between water uptake and ice nucleation by glassy organic aerosol particles, *Atmos. Chem. Phys.*, 2014, **14**, 12513–12531.

41 A. M. Arangio, J. H. Slade, T. Berkemeier, U. Pöschl, D. A. Knopf and M. Shiraiwa, Multiphase chemical kinetics of OH radical uptake by molecular organic markers of biomass burning aerosols: humidity and temperature dependence, surface reaction, and bulk diffusion, *J. Phys. Chem. A*, 2015, **119**, 4533–4544.

42 T. Berkemeier, A. Mishra, C. Mattei, A. J. Huisman, U. K. Krieger and U. Pöschl, Ozonolysis of Oleic Acid Aerosol Revisited: Multiphase Chemical Kinetics and Reaction Mechanisms, *ACS Earth Space Chem.*, 2021, **5**, 3313–3323.

43 P. S. J. Lakey, T. Berkemeier, M. Krapf, J. Dommen, S. S. Steimer, L. K. Whalley, T. Ingham, M. T. Baeza-Romero, U. Pöschl, M. Shiraiwa, M. Ammann and D. E. Heard, The effect of viscosity and diffusion on the HO_2 uptake by sucrose and secondary organic aerosol particles, *Atmos. Chem. Phys.*, 2016, **16**, 13035–13047.

44 A. C. Vander Wall, P. S. J. Lakey, E. Rossich Molina, V. Perraud, L. M. Wingen, J. Xu, D. Soulsby, R. B. Gerber, M. Shiraiwa and B. J. Finlayson-Pitts, Understanding interactions of organic nitrates with the surface and bulk of organic films: implications for particle growth in the atmosphere, *Environ. Sci.: Processes Impacts*, 2018, **20**, 1593–1610.

45 M. C. Fairhurst, M. J. Ezell, C. Kidd, P. S. Lakey, M. Shiraiwa and B. J. Finlayson-Pitts, Kinetics, mechanisms and ionic liquids in the uptake of n-butylamine onto low molecular weight dicarboxylic acids, *Phys. Chem. Chem. Phys.*, 2017, **19**, 4827–4839.

46 Y. Li, P. S. Lakey, M. J. Ezell, K. N. Johnson, M. Shiraiwa and B. J. Finlayson-Pitts, Distinct Temperature Trends in the Uptake of Gaseous n-Butylamine on Two Solid Diacids, *ACS EST Air*, 2023, **1**, 52–61.

47 P. Lakey, T. Berkemeier, M. T. T. Baeza-Romero, U. Pöschl, M. Shiraiwa and D. E. Heard, Towards a better understanding of the HO_2 uptake coefficient to aerosol particles measured during laboratory experiments, *Environ. Sci.: Atmos.*, 2024, **4**, 813–829.

48 W. Wang, X. Wang, P. S. Lakey, M. J. Ezell, M. Shiraiwa and B. J. Finlayson-Pitts, Gas phase and gas–solid interface ozonolysis of nitrogen containing alkenes: Nitroalkenes, enamines, and nitroenamines, *J. Phys. Chem. A*, 2022, **126**, 5398–5406.

49 B. Finlayson-Pitts, A. Anderson, P. Lakey, W. Wang, M. Ezell, X. Wang, L. Wingen, V. Perraud and M. Shiraiwa, Oxidation of solid thin films of neonicotinoid pesticides by gas phase hydroxyl radicals, *Environ. Sci.: Atmos.*, 2023, **3**, 124–142.

50 J. Socorro, P. S. J. Lakey, L. Han, T. Berkemeier, G. Lammel, C. Zetzsch, U. Pöschl and M. Shiraiwa, Heterogeneous OH Oxidation, Shielding Effects, and Implications for the Atmospheric Fate of Terbuthylazine and Other Pesticides, *Environ. Sci. Technol.*, 2017, **51**, 13749–13754.

51 M. Shiraiwa, U. Pöschl and D. A. Knopf, Multiphase Chemical Kinetics of NO3 Radicals Reacting with Organic Aerosol Components from Biomass Burning, *Environ. Sci. Technol.*, 2012, **46**, 6630–6636.

52 M. Shiraiwa, Y. Sosedova, A. Rouvière, H. Yang, Y. Zhang, J. P. Abbatt, M. Ammann and U. Pöschl, The role of long-lived reactive oxygen intermediates in the reaction of ozone with aerosol particles, *Nat. Chem.*, 2011, **3**, 291–295.

53 H. Deng, P. S. Lakey, Y. Wang, P. Li, J. Xu, H. Pang, J. Liu, X. Xu, X. Li and X. Wang, Daytime SO2 chemistry on ubiquitous urban surfaces as a source of organic sulfur compounds in ambient air, *Sci. Adv.*, 2022, **8**, eabq6830.

54 H. Fan, E. S. Frank, P. S. Lakey, M. Shiraiwa, D. J. Tobias and V. H. Grassian, Heterogeneous Interactions between Carvone and Hydroxylated SiO_2, *J. Phys. Chem. C*, 2022, **126**, 6267–6279.

55 Y. Fang, P. Lakey, S. Riahi, A. McDonald, M. Shrestha, D. J. Tobias, M. Shiraiwa and V. Grassian, A Molecular Picture of Surface Interactions of Organic Compounds on Prevalent Indoor Surfaces: Limonene Adsorption on SiO_2, *Chem. Sci.*, 2019, **10**, 2906–2914.

56 H. Fan, P. S. Lakey, E. S. Frank, D. J. Tobias, M. Shiraiwa and V. H. Grassian, Comparison of the Adsorption–Desorption Kinetics of Limonene and Carvone on TiO_2 and SiO_2 Surfaces under Different Relative Humidity Conditions, *J. Phys. Chem. C*, 2022, **126**, 21253–21262.

57 J. Liu, H. Deng, P. S. Lakey, H. Jiang, M. Mekic, X. Wang, M. Shiraiwa and S. Gligorovski, Unexpectedly High Indoor HONO Concentrations Associated with Photochemical NO_2 Transformation on Glass Windows, *Environ. Sci. Technol.*, 2020, **54**, 15680–15688.

58 S. Zhou, B. C. Hwang, P. S. Lakey, A. Zuend, J. P. Abbatt and M. Shiraiwa, Multiphase reactivity of polycyclic aromatic hydrocarbons is driven by phase separation and diffusion limitations, *Proc. Natl. Acad. Sci. U.S.A.*, 2019, **116**, 11658–11663.

59 Z. Zhou, P. S. Lakey, M. von Domaros, N. Wise, D. J. Tobias, M. Shiraiwa and J. P. Abbatt, Multiphase Ozonolysis of Oleic Acid-Based Lipids: Quantitation of Major Products and Kinetic Multilayer Modeling, *Environ. Sci. Technol.*, 2022, **56**, 7716–7728.

60 G. Morrison, P. S. Lakey, J. Abbatt and M. Shiraiwa, Indoor boundary layer chemistry modeling, *Indoor Air*, 2019, **29**, 956–967.

61 M. Shiraiwa and U. Pöschl, Mass accommodation and gas–particle partitioning in secondary organic aerosols: dependence on diffusivity, volatility, particle-phase reactions, and penetration depth, *Atmos. Chem. Phys.*, 2021, **21**, 1565–1580.

62 P. S. J. Lakey, G. C. Morrison, Y. Won, K. M. Parry, M. von Domaros, D. J. Tobias, D. Rim and M. Shiraiwa, The impact of clothing on ozone and squalene ozonolysis products in indoor environments, *Commun. Chem.*, 2019, **2**, 56.

63 P. S. Lakey, A. Zuend, G. C. Morrison, T. Berkemeier, J. Wilson, C. Arata, A. H. Goldstein, K. R. Wilson, N. Wang and J. Williams, Quantifying the impact of relative humidity on human exposure to gas phase squalene ozonolysis products, *Environ. Sci.: Atmos.*, 2023, **3**, 49–64.

64 Y. Won, P. S. Lakey, G. Morrison, M. Shiraiwa and D. Rim, Spatial Distributions of Ozonolysis Products From Human Surfaces In Ventilated Rooms, *Indoor Air*, 2020, **30**, 1229–1240.

65 A. K. Hua, P. S. Lakey and M. Shiraiwa, Multiphase kinetic multilayer model interfaces for simulating surface and bulk chemistry for environmental and atmospheric chemistry teaching, *J. Chem. Educ.*, 2022, **99**, 1246–1254.

66 A. Milsom, A. Lees, A. M. Squires and C. Pfrang, MultilayerPy (v1. 0): a Python-based framework for building, running and optimising kinetic multi-layer models of aerosols and films, *Geosci. Model Dev.*, 2022, **15**, 7139–7151.

67 R. Alwarda, S. Zhou and J. P. Abbatt, Heterogeneous oxidation of indoor surfaces by gas-phase hydroxyl radicals, *Indoor Air*, 2018, **28**, 655–664.

68 C. M. A. Eichler, Y. Wu, J. Cao, S. Shi and J. C. Little, Equilibrium relationship between SVOCs in PVC products and the air in contact with the product, *Environ. Sci. Technol.*, 2018, **52**, 2918–2925.

69 Y. Wu, C. M. A. Eichler, W. Leng, S. S. Cox, L. C. Marr and J. C. Little, Adsorption of phthalates on impervious indoor surfaces, *Environ. Sci. Technol.*, 2017, **51**, 2907–2913.

70 C. J. Weschler and W. W. Nazaroff, Growth of organic films on indoor surfaces, *Indoor Air*, 2017, **27**, 1101–1112.

71 P. S. J. Lakey, A. Wisthaler, T. Berkemeier, T. Mikoviny, U. Pöschl and M. Shiraiwa, Chemical kinetics of multiphase reactions between ozone and human skin lipids: implications for indoor air quality and health effects, *Indoor Air*, 2017, **27**, 816–828.

72 R. Sander, Compilation of Henry's law constants (version 5.0. 0) for water as solvent, *Atmos. Chem. Phys.*, 2023, **23**, 10901–12440.

73 M. von Domaros, P. S. Lakey, M. Shiraiwa and D. J. Tobias, Multiscale Modeling of Human Skin Oil-Induced Indoor Air Chemistry: Combining Kinetic Models and Molecular Dynamics, *J. Phys. Chem. B*, 2020, **124**, 3836–3843.

74 M. Tang, M. Shiraiwa, U. Pöschl, R. Cox and M. Kalberer, Compilation and evaluation of gas phase diffusion coefficients of reactive trace gases in the atmosphere: Volume 2. Diffusivities of organic compounds, pressure-normalised mean free paths, and average Knudsen numbers for gas uptake calculations, *Atmos. Chem. Phys.*, 2015, **15**, 5585–5598.

75 M. Tang, R. Cox and M. Kalberer, Compilation and evaluation of gas phase diffusion coefficients of reactive trace gases in the atmosphere: volume 1. Inorganic compounds, *Atmos. Chem. Phys.*, 2014, **14**, 9233–9247.

76 J. Vieceli, M. Roeselova, N. Potter, L. X. Dang, B. C. Garrett and D. J. Tobias, Molecular dynamics simulations of atmospheric oxidants at the air– water interface: solvation and accommodation of OH and O_3, *J. Phys. Chem. B*, 2005, **109**, 15876–15892.

77 T. F. Wang, G. B. Kasting and J. M. Nitsche, A multiphase microscopic diffusion model for stratum corneum permeability. II. Estimation of physicochemical parameters, and application to a large permeability database, *J. Pharm. Sci.*, 2007, **96**, 3024–3051.

78 Y. Dancik, M. A. Miller, J. Jaworska and G. B. Kasting, Design and performance of a spreadsheet-based model for estimating bioavailability of chemicals from dermal exposure, *Adv. Drug Delivery Rev.*, 2013, **65**, 221–236.

79 T. Berkemeier, M. Ammann, U. K. Krieger, T. Peter, P. Spichtinger, U. Pöschl, M. Shiraiwa and A. J. Huisman, Technical note: Monte Carlo genetic algorithm (MCGA) for model analysis of multiphase chemical kinetics to determine transport and reaction rate coefficients using multiple experimental data sets, *Atmos. Chem. Phys.*, 2017, **17**, 8021–8029.

80 J. Wei, T. Fang, C. Wong, P. S. Lakey, S. A. Nizkorodov and M. Shiraiwa, Superoxide formation from aqueous reactions of biogenic secondary organic aerosols, *Environ. Sci. Technol.*, 2020, **55**, 260–270.

81 D. Rim, E. T. Gall, S. Ananth and Y. Won, Ozone reaction with human surfaces: Influences of surface reaction probability and indoor air flow condition, *Build. Env.*, 2018, **130**, 40–48.

82 Y. Wu, C. M. Eichler, W. Leng, S. S. Cox, L. C. Marr and J. C. Little, Adsorption of phthalates on impervious indoor surfaces, *Environ. Sci. Technol.*, 2017, **51**, 2907–2913.
83 P. S. J. Lakey, Y. Won, D. Shaw, F. F. Østerstrøm, J. Mattila, E. Reidy, B. Bottorff, C. Rosales, C. Wang, L. Ampollini, S. Zhou, A. Novoselac, T. F. Kahan, P. F. DeCarlo, J. P. D. Abbatt, P. S. Stevens, D. K. Farmer, N. Carslaw, D. Rim and M. Shiraiwa, Spatial and temporal scales of variability for indoor air constituents, *Commun. Chem.*, 2021, **4**, 110.
84 S. Yang and D. Licina, Nanocluster aerosol formation via ozone chemistry on worn clothing: Influence of environmental parameters, *Build. Env.*, 2024, **256**, 111474.
85 S. Yang, D. Licina, C. J. Weschler, N. Wang, N. Zannoni, M. Li, J. Vanhanen, S. Langer, P. Wargocki and J. Williams, Ozone initiates human-derived emission of nanocluster aerosols, *Environ. Sci. Technol.*, 2021, **55**, 14536–14545.
86 S. Yang, T. Müller, N. Wang, G. Bekö, M. Zhang, M. Merizak, P. Wargocki, J. Williams and D. Licina, Influence of Ventilation on Formation and Growth of 1–20 nm Particles via Ozone–Human Chemistry, *Environ. Sci. Technol.*, 2024, **58**, 4704–4715.
87 D. Shaw and N. Carslaw, INCHEM-Py: An open source Python box model for indoor air chemistry, *J. Open Source Softw.*, 2021, **6**, 3224.
88 D. R. Shaw, T. J. Carter, H. L. Davies, E. Harding-Smith, E. C. Crocker, G. Beel, Z. Wang and N. Carslaw, INCHEM-Py v1. 2: A community box model for indoor air chemistry, *Geosci. Model Dev.*, 2023, **16**, 7411–7431.
89 B. E. Cummings, P. S. Lakey, G. C. Morrison, M. Shiraiwa and M. S. Waring, Composition of indoor organic surface films in residences: simulating the influence of sources, partitioning, particle deposition, and air exchange, *Environ. Sci.: Processes Impacts*, 2024, **26**, 305–322.
90 Y. Liu, P. K. Misztal, C. Arata, C. J. Weschler, W. W. Nazaroff and A. H. Goldstein, Observing ozone chemistry in an occupied residence, *Proc. Natl. Acad. Sci. U.S.A.*, 2021, **118**, e2018140118.